JOURNAL OF MATERIALS SCIENCE 28 (1993) 6496–6502

Evolution of morphology in high molecular weight polyethylene during die drawing

JIANXIONG LI*, YEW-WING LEE
Department of Manufacturing Engineering, Hong Kong Polytechnic Hung Hom, Kowloon, Hong Kong

Deformed high molecular weight polyethylene (HMWPE) rod, formed by die drawing at 115 °C, was cleaved longitudinally at liquid nitrogen temperature and the cleaved surface was etched by the permanganic etching technique. A series of etched surfaces of HMWPE sections of variable draw ratio (1–13) was analysed by scanning electron microscopy (SEM). The evolution of crystalline structure in HMWPE during die drawing was observed directly. In undrawn HMWPE, the spherulites were made up of sheaf-like lamellae and scattered within an amorphous phase. During die drawing, first, microscopically inhomogeneous deformation occurred and the spherulites aligned along the drawing direction; then at a draw ratio of about 7, local melting occurred, the spherulites disintegrated and the sheaf-like lamellae oriented, followed by strain-induced recrystallization and the growth of the lamellae; finally, at a draw ratio of about 12, plastic deformation of the lamellae occurred and microfibrils were formed by drawing the lamellae.

1. Introduction

Semicrystalline polymers can be processed below their melting points and oriented preferentially, thus improving their strength and moduli in the orientation direction drastically [1–3]. Although this characteristic response of semicrystalline polymers is well known, and indeed is often exploited in solid-phase polymeric processing such as tensile drawing [4, 5], solid-state extrusion [6], and die drawing [7–9], it is not yet well understood. The strain-hardening response of semicrystalline polymers is usually accompanied by the transformation of initially isotropic melt-crystallized semicrystalline polymers into a fibrous structure [10, 11]. It is generally recognized that isotropic semicrystalline polymers become fibrous when they are drawn to yielding, but the process of the transformation during drawing is still not very clear. In the most commonly quoted model suggested by Peterlin [12–14], the process has been described on the basis of rotation of the lamellae, phase-transformation twinning, chain-tilting, slip and final disintegration of the lamellae into small chain-folded blocks built into a "shish-kebab" structure of microfibrils. This model implies that the long period in the fibrous structure should be close to that in the undrawn materials. However, the fact is that for drawn polyethylene the long period is dependent on draw temperature [15, 16] and, in some cases, the small-angle X-ray scattering long-period peak intensity decreases and even disappears, and this can be interpreted in several ways [17, 18]. Hendra *et al.* suggested there was some sort of local melting and recrystallization to enrich Peterlin's model [19]. However, these hypotheses have not been verified directly, the process of the transformation from spherulite to microfibril has not been observed directly for bulk specimens. The major bar to the resolution of this problem is the absence of a suitable method by which a qualified specimen can be prepared from the bulk semicrystalline polymers for direct observation of the detailed morphology.

In the past, transmission electron microscopy of thin films has been necessary for the direct observation of morphological change [20, 21]. Thin films, however, are generally subject to a different stress regime and might deform differently from the bulk. Additionally, because thermal conductivity of the polymers is poor, the bulk might suffer from "heat build-up" due to its inability to disperse effectively the heat during processing. For melt-crystallized polyethylene sheets, local melting has been probed by the neutron scattering technique [22, 23]. Therefore, it is believed that the mechanism of deformation in bulk specimens is different from that in thin films.

The development of the permanganic etching technique by Olley *et al.* [24] permits the direct observation of the fine details of the lamellar morphology in various polyethylene [24–31] and polypropylene [24, 31, 32] bulk specimens, in contrast to the extensive earlier studies on thin films. However, direct observation of the evolution of crystalline structure in semicrystalline polymers during deformation has not been reported.

This paper reports the results of direct observation of the crystalline structure for the drawn high molecular weight polyethylene (HMWPE) specimen prepared

Present address: Department of Mechanical Engineering, University of Hong Kong, Poktalam Road, Hong Kong.

0022–2461

by the permanganic acid etching technique, and shows the details of the transformation of crystalline structure from spherular to microfibrillar for HMWPE during die drawing up to a draw ratio of 13.

2. Experimental procedure

2.1. Materials

The material investigated in this study was high molecular weight polyethylene supplied in bar stock form produced by melt extrusion. It was known from the local supplier that the average molecular weight was about 50×10^4. The density, melting point and melt flow index were measured to be 0.948 g cm^{-3}, 132–134 °C and 0.20 g/10 min, respectively.

2.2. Die drawing

Die drawing was performed on an Instron 4301 Materials Testing Machine following the procedure described by Ward and Coates [7]. The billet with a diameter of 25 mm was drawn through a conical die with 7.2 mm die exit at 25 mm min^{-1} draw speed. During drawing the temperature of the die, the billet and the aluminium block was maintained at 115 °C. When about 100 mm length of billet had been drawn through the die, the drawing process was terminated and the billet was permitted to cool under tension. After the billet temperature had dropped to below 50 °C, the tension was relieved and the billet was taken out. The undeformed, deformed and drawn portions of the billet were used for morphological observation. In order to observe the changes of morphology in bulk HMWPE during die drawing, the remnants of the billet and the drawn product were cleaved longitudinally at liquid nitrogen temperature and the cleaved surfaces were treated with permanganic etchant and observed with a scanning electron microscope (SEM).

2.3. Surface etching

The permanganic acid etching technique adopted in this work was similar to that described by Naylor and Phillips [30] but with some modifications. The etchant used was a solution of 0.5 % (wt/wt) potassium permanganate in 95 % sulphuric acid, the etching and washing processes were performed under an ultrasonic bath. First, the cleaved surface was etched at 28–32 °C for 120 min in a 50 ml beaker containing 30 ml etchant and the etched specimen was washed with 30 % sulphuric acid, 30 % hydrogen peroxide, distilled water and finally acetone, as described by Olley *et al.* [24]. Then the etched specimen was immersed in 30 % hydrogen peroxide at 4 °C for 4 h. Finally the etched surface was re-etched twice at about 4 °C and was re-washed.

2.4. Scanning electron microscopy

The etched surface of the specimen was coated with a gold layer in a Polaron SEM Autocoating Unit E5200. Altogether nine runs were used to coat the gold layer, a coating period of 20 s was employed in each run to avoid any damage to the morphology of the fine lamellae caused by coating. A sequence of sections on the treated surfaces in the remnant billet and the drawn products was observed in a Cambridge S250 scanning electron microscope.

3. Results

3.1. Morphology of the undrawn billet

Fig. 1 shows electron micrographs of the lightly etched surface in the undrawn billet, i.e. it was etched at 20 °C for 2 h only. The undrawn billet has a typical spherulite structure [33] as can be seen in Fig. 1a. The average sizes of the spherulites are about 40 μm, with a maximum size of about 60 μm and a minimum of about 15 μm. The spherulites are scattered randomly. In some cases when the cleaving plane had just passed through the core of a spherulite, the sheaf-like [25, 26, 32, 33] structure of the spherulite can be seen, as shown in Fig. 1b. The lamellae in the sheaf have a thickness of about 120 nm and a length of 2–3 μm (Fig. 1c, d). The appearance of the lamellae presents in S-shape and the main axes of the sheaf-like lamellae seem to orient randomly. Fig. 1c also reveals the boundary areas between the spherulites in the undrawn billet. In these areas, the lamellae are relatively rare and much shorter than those in the sheaf-like structure, the core of spherulites, having a length of about 0.2–0.7 μm, but still maintain a thickness of about 120 nm. However, in the core of the spherulite, the lamellae are stacked fairly compactly as shown in Fig. 1d.

3.2. Morphology of the deformed billet

This study addresses the evolution of crystalline phase morphology in HMWPE during die drawing. In order to expose the change to the spherulites and the lamellae at the same time, the cleaved surface of the deformed billet was etched first at room temperature and then immersed in 30 % hydrogen peroxide and finally was re-etched at low temperature. Fig. 2 indicates the locations of a series of portions observed on the treated surface along the drawing direction. Portion A is the region at which the deformation of the billet has just begun; at Portion B, the billet has been drawn to a draw ratio of 2; and at Portion C, the billet has reached the draw ratio of about 4, and the billet begins to become transparent. At Portion D, the draw ratio of the billet is about 7; Portion E is at the exit of the die and the draw ratio is about 12.6.

Fig. 3 shows an electron micrograph taken in Portion A. The morphology of the spherulite in this portion resembles that in the undrawn billet in size and distribution (refer to Fig. 1a) except that the boundary between the spherulites has been preferentially etched away. The spherulites with a diameter ranging from 15–60 μm are also scattered randomly. In fact, the deformation of the billet in this portion was slight, hence the morphology of the spherulite should be similar to that in the undrawn billet.

Fig. 4 shows electron micrographs taken in Portion B, at which the billet had been drawn to a draw ratio

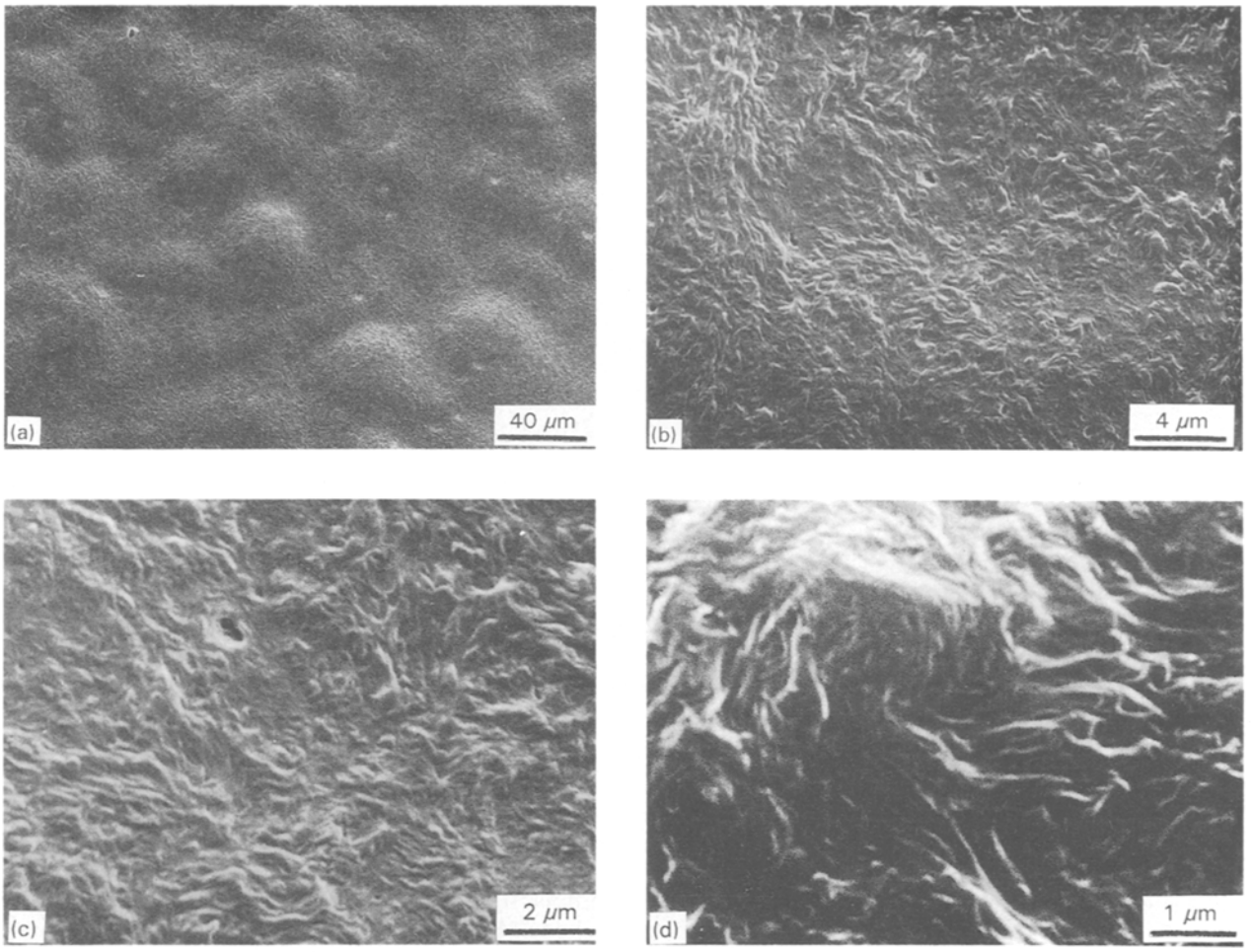

Figure 1 Electron micrographs of the undrawn HMWPE billet. (a) a view of the spherulites in the undrawn billet, (b, c) the sheaf-like lamellae in the spherulite, (d) the core of the spherulite.

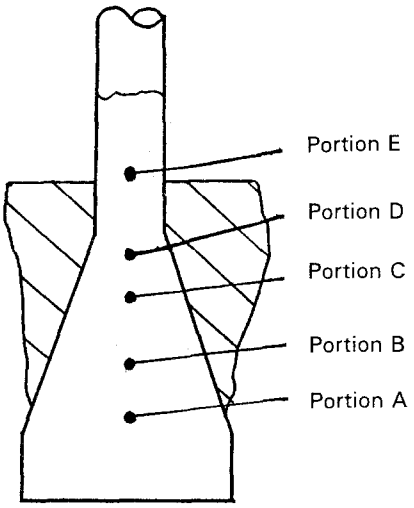

Figure 2 Location of the series of portions to be observed on the remnant of the billet.

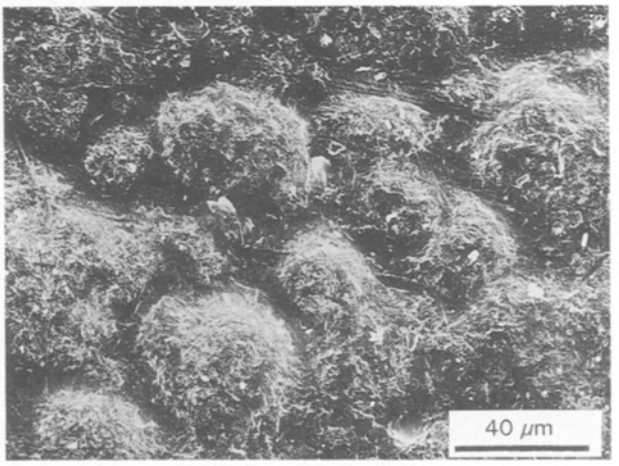

Figure 3 Electron micrograph of Portion A which was deeply etched. The drawing direction is downwards.

of about 2. In this portion the diameters of the spherulites still range from 15–60 μm, but the spherulites seem to have aligned along the drawing direction and have not deformed distinctly as shown in Fig. 4a. Fig. 4b shows an electron micrograph of the boundary areas between the spherulites. Compared to that in the undrawn billet (Fig. 1c), the lamellae between the spherulites seem to have increased in dimension and in quantity, and in addition the lamellae have some small "spherulites" emerging, which have a size of about 0.7 μm. This may be the result of local melting during die drawing and then recrystallization during cooling. Although the spherulites in this portion begin to align, the lamellae between the spherulites still orient randomly.

Fig. 5 shows electron micrographs taken in Portion C, at which the billet has been drawn to a draw ratio of about 4. In this portion the spherulites have arranged

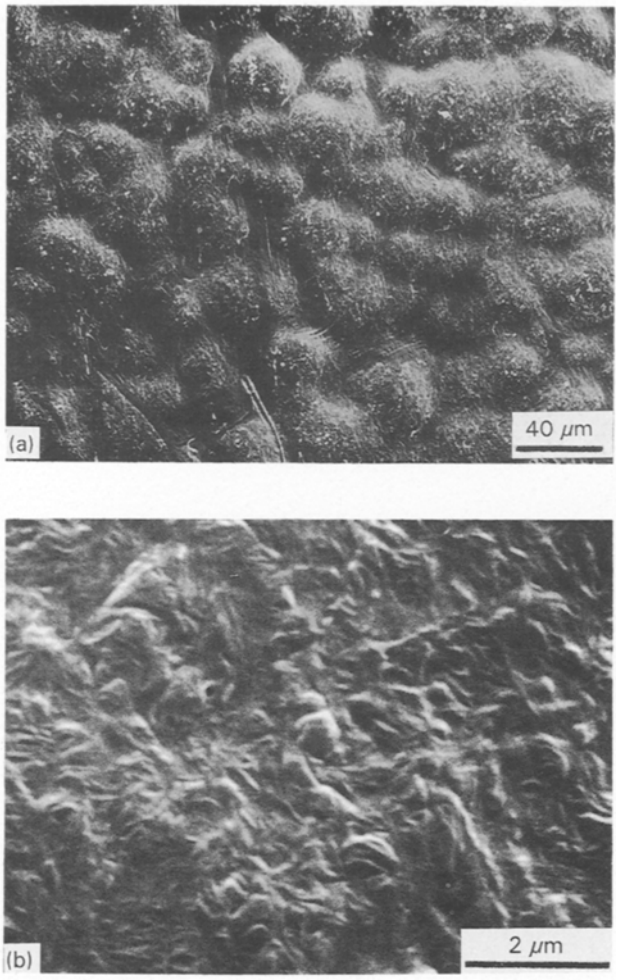

Figure 4 Electron micrographs of deformed HMWPE billet at a draw ratio of 2. The drawing direction is downwards. (a) The arrangement of the spherulites in the deformed billet, (b) a view of the boundary area between the spherulites.

in rows along the drawing direction (Fig. 5a, b). The average dimension of the spherulites seems to decrease distinctly, i.e. the number of spherulites with smaller diameters has increased. Fig. 5c shows an enlarged view of the texture between the spherulites: the texture is rather different from that in Portion B (Fig. 4b). In this portion the lamellae became thicker and longer, and the S-shaped lamellae began orientation although there are some smaller unoriented lamellae that resemble those in Portion B (Fig. 4b). This might be due to the disintegration of some small spherulites and the strain-induced crystallization during die drawing.

The morphology in Portion D is shown in Fig. 6. Portion D was situated near the neck of the die, at which the billet had been drawn to a draw ratio of about 7 and had become fairly transparent. In this portion the structure of the crystal has changed substantially. Complete spherulites are now almost absent, the spherulites arranged in rows become vague and begin to disappear. There are clear tracks of melt flow along the drawing direction (Fig. 6a). Further drawing results in complete disappearance of the spherulites (Fig. 6b). Fig. 6c shows enlarged detail of the morphology in Fig. 6b. When the billet has been drawn to this stage, the spherulites have completely disintegrated, leaving the S-shaped lamellae. Some of

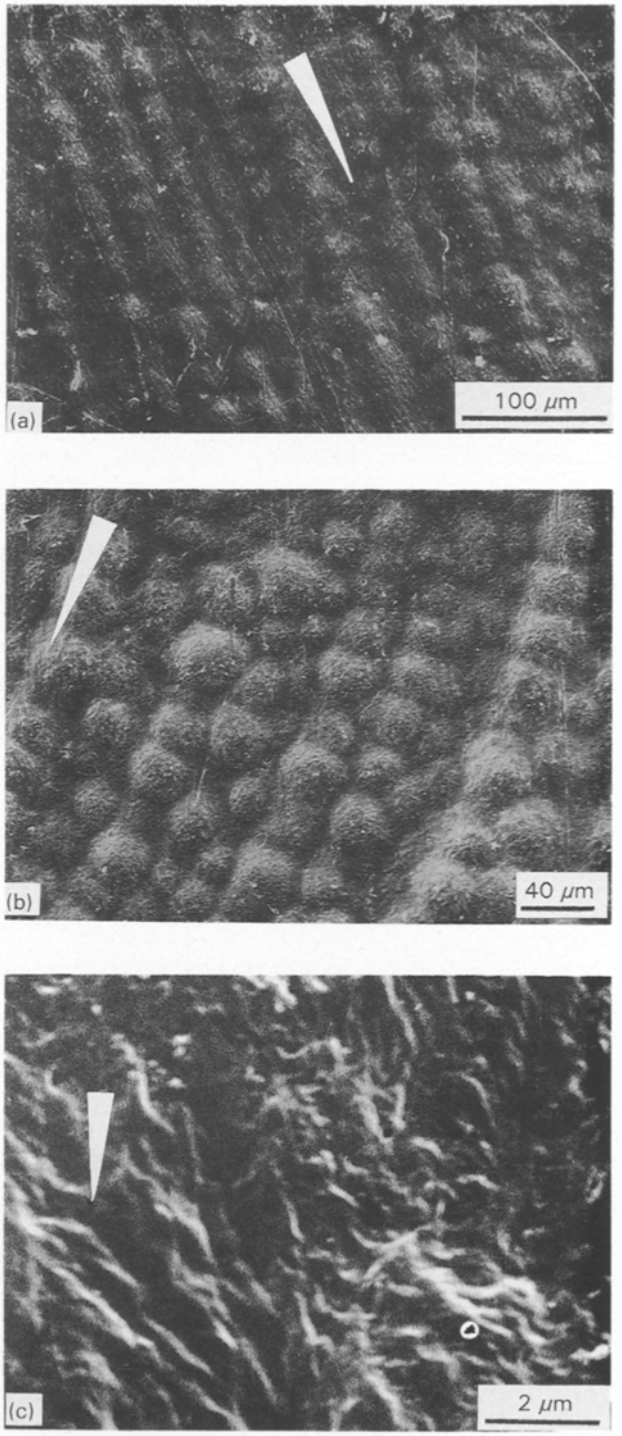

Figure 5 Electron micrographs of deformed HMWPE billet at a draw ratio of 4. The draw direction is indicated by the arrow. (a, b) The arrangement in rows of the spherulites in the deformed billet, (c) a view of the boundary area between the rows.

the lamellae coalesce laterally and form sheaf-lamellae, which are oriented in the drawing direction. Although the majority of the lamellae are oriented preferentially, there are some short lamellae lying randomly as shown on the right-hand side of Fig. 6d. Compared to that in the undrawn HMWPE, the lamellae become longer, thicker and more compact; the lamellae can be as long as 5 μm. In general, the longer lamellae tend to orient in the drawn direction. It is believed that this is the result of local melting and strain-induced crystallization.

Fig. 7 shows the electron micrographs taken in Portion E, at which the billet had been just drawn out

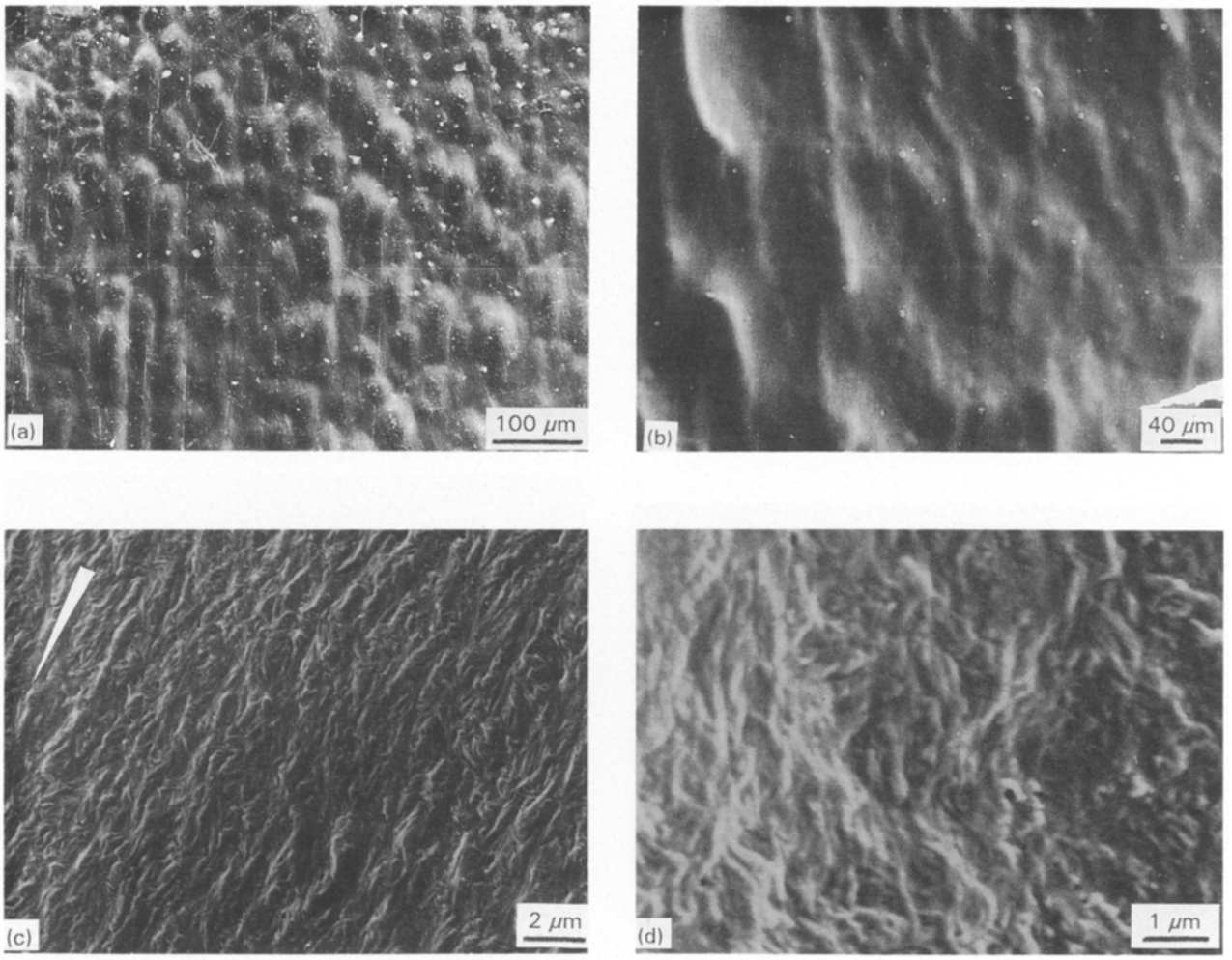

Figure 6 Electron micrographs of deformed HMWPE billet at a draw ratio of about 7. The draw direction is downwards. (a) The melt flow and disintegration of the spherulites in the deformed billet at a draw ratio of 6, (b) the disintegration of the spherulites in the billet at a draw ratio of 7.5, (c) an enlarged view of (b) showing the oriented sheaf-like lamellae, (d) details of the lamellae.

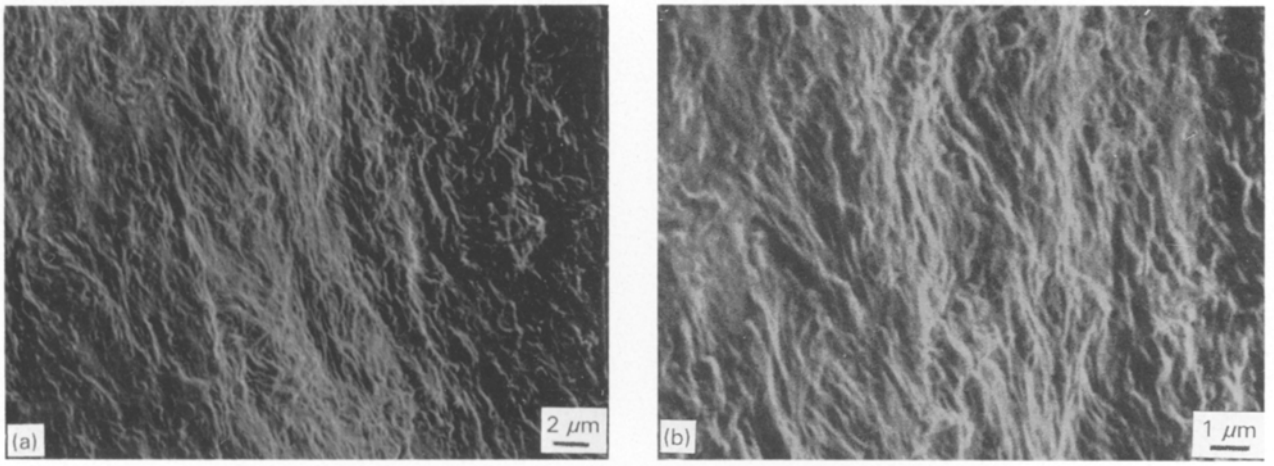

Figure 7 Electron micrographs of a drawn portion at the exit of the die with a draw ratio of about 12.5, showing the micella microfibrils, the embryo of the microfibril. The drawing direction is downwards.

of the exit of the die and the draw ratio was approximately 12.6. In this portion the morphology has developed further. In addition to more oriented lamellae, a new category of structure emerges, which can be termed "micella microfibrils", or "embryo" of the microfibrils. These microfibrils are about 200 nm in width, assume sheaves and still retain some degree of S-shaping. It is clear that they were formed by drawing the oriented lamellae in the sheaf-like structure.

3.3. Morphology of the drawn products

Fig. 8 is an electron micrograph of the drawn product, which has a draw ratio of about 12.6 and is located at a distance of about 100 mm from the exit of the die. Compared to that at the exit of the die (Portion E, Fig. 7) the morphology has undergone a drastic change. The S-shaped lamellae have vanished completely and the overall morphology is fibrous; however, a few vestiges of S-shaped lamellae still remain;

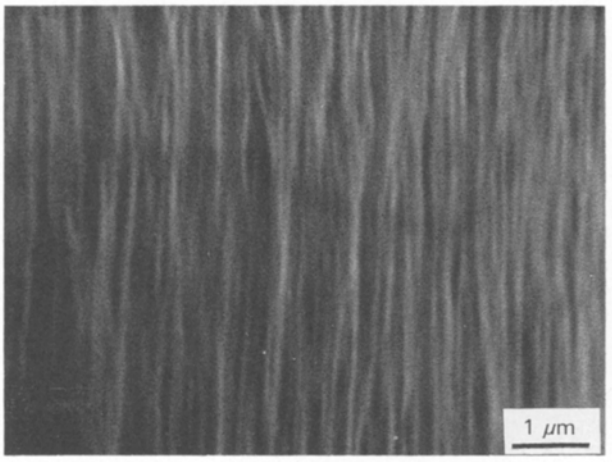

Figure 8 Electron micrographs of a drawn portion with a draw ratio of about 12.6 located at a distance of about 100 mm from the exit of the die. The drawing direction is downwards.

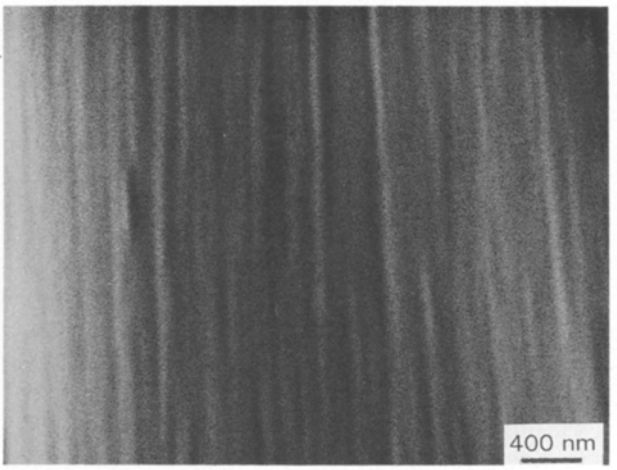

Figure 9 Electron micrographs of a drawn portion with a draw ratio of about 12.6 located at a distance of about 200 mm from the exit of the die. The drawing direction is downwards.

the microfibril exhibits slight meandering. The diameters of the microfibrils have been drawn to about 130 nm from 200 nm, as mentioned in the previous paragraph (refer to Fig. 7).

Fig. 9 shows electron micrographs of the final product, which has a three-point bend modulus of about 16 GPa and is located at a distance of about 200 mm from the exit of the die. The morphology of the final product appears to be very fibrous. The microfibrils have been drawn to a diameter of about 70 nm, and extend straight along the drawing direction; they coalesce laterally and a few amorphous materials are embedded between them, whereas individual microfibrils appears to be structurally similar to needle-like crystals.

4. Discussion

The sequence of micrographs presented has delineated the crystalline structure of HMWPE and its evolution from spherulite to microfibril during die drawing.

In the undrawn HMWPE billet, the lamellae are the basic element which stack compactly in the manner of sheaf-like structures, as described by Bassett [32, 33] and constitute the spherulites (Fig. 1). The organized spherulites are scattered among the disorganized amorphous materials; so the inter-spherulitic materials can be preferentially etched away leaving behind the organized spherulites when the specimen has been etched deeply (Fig. 3). Although the inter-spherulite materials are less organized, they contain a few short lamellae, which are embedded in amorphous materials, but the quantity is relatively small (Fig. 1b, c).

When the draw stress acted on the billet, microscopically inhomogeneous deformation occurred in the billet; the inter-spherulite materials produced a larger strain because the major inter-spherulite materials are amorphous and have a lower modulus than the spherulites. In addition, die drawing was performed at elevated temperature; owing to the thermomechanical effect, the short lamellae on the boundary of the spherulites partially melt, thus the draw stress could rearrange the spherulites into rows. This is a response to the decrease in spherulite size at the time of alignment of the spherulites (Fig. 5b).

When the billet was drawn to a draw ratio of about 4, the alignment of the spherulites was completed; further drawing resulted in the disintegration of spherulites and the transformation of spherulite to fibril (Figs 6–8). This transformation began at a draw ratio of about 7. Because of this transformation, the dimension of the crystal phase decreased from 40 μm (spherulites) to 200 nm (lamellae), which is shorter than the wavelength of visible light waves, so that the billet became fairly transparent when the billet was drawn to this draw ratio.

The transformation had undergone a process of local melting, strain-induced crystallization, plastic deformation of lamellae, and finally formation of microfibrils. At a draw ratio of about 7 the spherulites were broken up completely and left the sheaf-like lamellae oriented along the drawing direction (Fig. 6c). Under the effect of strain-induced crystallization, the lamellae grew in length (Fig. 6c, d). Further drawing made the lamellae extend, straighten, lengthen and thin gradually (Figs 7–9). At a draw ratio of about 12, the S-shaped lamellae were drawn into micella microfibrils (Fig. 7), and then the micella microfibrils became longer and thinner on drawing, and finally transformed into microfibrils (Figs 8 and 9).

The process of deformation observed in this work is slightly different from that described by Peterlin. In Peterlin's model, the process of deformation is divided into three stages: the plastic deformation of spherulites, the transformation from spherulite to fibril, and plastic deformation of fibril. The transformation is envisaged as the breaking away of small blocks of crystals from lamellar stacks in unoriented materials, and subsequent reorientation and restacking to form microfibrils of oriented materials. However, in the present study, the plastic deformation of spherulites has not been identified, only the alignment of the spherulites at the low draw ratio, and local melting and strain-induced recrystallization at a draw ratio of about 7 have been observed.

The crystalline structure in the final product is the laterally coalesced microfibrils, between which some non-crystalline amorphous materials are embedded. The "shish-kebab" structure, alternating amorphous and crystalline layers, which is considered to be the characteristic structure of the microfibril [18, 33], has not been observed. This may be due to the limitation of amplification for the direct observation of specimens by SEM, or the fact that the microfibril is a continuous crystalline phase which was formed by a strain-induced recrystallization. The latter may be true, because for the drawn PE, the SAXS long-period intensity decreases and even disappears when the draw ratio exceeds 10 [17, 18], which corresponds to the process of the formation of microfibrils observed in this study (Figs 6 and 7). Detailed elucidation of the structure of the microfibrils and the structural changes outlined here will require further investigation.

5. Conclusion

The crystalline structure of the undrawn HMWPE billet is a typical spherulitic structure which is made up of sheaf-like lamellae scattered among the amorphous material. During die drawing, the crystalline structure evolves as follows:

1. plastic deformation of inter-spherulite materials and alignment of spherulites;
2. local melting, disintegration of spherulites and orientation of sheaf-like lamellae;
3. strain-induced crystallization and growth of lamellae;
4. plastic deformation of S-shaped lamellae and formation of microfibrils by drawing the lamellae.

The crystalline structure of the final drawn products consists of laterally coalesced microfibrils, between which some amorphous materials are embedded.

Acknowledgement

The authors thank Mrs Sni-Ling Wong, Department of Applied Physics, Hong Kong Polytechnic, for assistance with preparation of the scanning electron micrographs.

References

1. D. M. BIGG, *Polym. Eng. Sci.* **28** (1988) 830.
2. A. PETERLIN, *Colloid Polym. Sci.* **265** (1987) 357.
3. L. H. WANG and R. S. PORTER, *Polym. Commun.* **31** (1990) 457.
4. W. H. CAROTHERS and J. W. HILL, *J. Am. Chem. Soc.* **54** (1932) 1566.
5. *Idem, ibid.* **54** (1932) 1579.
6. S. KOJIMA and R. S. PORTER, *J. Polym. Sci. Polym. Phys. Edn.* **16** (1978) 1729.
7. I. M. WARD and P. D. COATES, *Polymer* **20** (1979) 1553.
8. A. K. TARAIYA, A. RICHARDSON and I. M. WARD, *J. Appl. Polym. Sci.* **33** (1987) 2559.
9. A. SELWOOD, B. PARSONS and I. M. WARD, *Plast. Rubber Proc. Applic.* **4** (1989) 229.
10. J. STEIDL and Z. PELZBAUER, *J. Polym. Sci. (C)* (1972) 345.
11. A. G. GIBSON, I. M. WARD, B. N. COLE and B. PARSONS, *J. Mater. Sci.* **9** (1974) 1193.
12. A. PETERLIN, *ibid.* **6** (1971) 490.
13. *Idem, J. Polym. Sci. (C)* **9** (1965) 61.
14. *Idem, ibid.* **10** (1966) 427.
15. A. PETERLIN and F. BALTA-CALLEJA, *J. Colloid Polym. Sci.* **242** (1970) 1093.
16. C. J. FARRELL and A. KELLER, *J. Mater. Sci.* **12** (1977) 966.
17. W. W. ADAMS, R. M. BRIBER, E. S. SHERMAN, R. S. PORTER and E. L. THOMAS, *Polymer* **26** (1985) 7.
18. W. W. ADAMS, D. YANG and E. L. THOMAS, *J. Mater. Sci.* **21** (1986) 2239.
19. P. J. HENDRA, H. WILLIAM and M. TAYLOR, *Polymer* **26** (1985) 1501.
20. P. M. TARIN and E. L. THOMAS, *Polym. Eng. Sci.* **19** (1979) 1017.
21. *Idem, ibid.* **18** (1978) 472.
22. D. M. SADLER and P. BARHAM, *J. Polymer* **31** (1990) 36.
23. *Idem, ibid.* **31** (1990) 43.
24. R. H. OLLEY, A. M. HODGE and D. C. BASSETT, *J. Polym. Sci. Polym. Phys. Edn.* **17** (1979) 627.
25. R. M. GOHIL and P. J. PHILLIPS, *Polymer* **27** (1986) 1687.
26. *Idem, ibid.* **27** (1986) 1696.
27. P. J. PHILLIPS and R. J. PHILOT, *Polym. Commun.* **27** (1986) 307.
28. D. R. NORTON and A. KELLER, *J. Mater. Sci.* **19** (1984) 447.
29. P. E. REED, and G. Q. ZHAO, *ibid.* **17** (1982) 3327.
30. K. L. NAYLOR and P. J. PHILLIPS, *J. Polym. Sci. Polym. Phys. Edn.* **21** (1983) 2011.
31. N. V. BHAT, R. J. HOWE and D. M. SHINOZAKI, *J. Polym. Mater.* **7** (1990) 41.
32. D. R. NOYTON and A. KELLER, *Polymer* **26** (1985) 704.
33. D. C. BASSETT, "Principles of Polymer Morphology" (Cambridge University Press, 1981).

Received 27 April 1992
and accepted 24 February 1993